Inorg. Chem. **2006**, *45*, 10066–10076

Trinuclear Copper(II) Complexes Derived from Schiff-Base Ligands Based on a 6-Amino-6-deoxyglucopyranoside: Structural and Magnetic Characterization

Arne Roth,[†] Jana Becher,[‡] Carmen Herrmann,[§] Helmar Görls,[†] Gavin Vaughan,[¶] Markus Reiher,[§] Dieter Klemm,[‡] and Winfried Plass*,[†]

Institut für Anorganische und Analytische Chemie, Friedrich-Schiller-Universität Jena, Carl-Zeiss-Promenade 10, D-07745 Jena, Germany, Institut für Organische Chemie und Makromolekulare Chemie, Friedrich-Schiller-Universität Jena, Humboldtstrasse 10, D-07743 Jena, Germany, Laboratorium für Physikalische Chemie, ETH Zürich, Hönggerberg Campus, Wolfgang-Pauli-Strasse 10, CH-8093 Zürich, Switzerland, and European Synchrotron Radiation Facility (ESRF), BP220, 38043 Grenoble Cedex, France

Received March 26, 2006

The trinuclear copper(II) complexes ([Cu**L1**)(μ-ac)Cu(μ-ac)Cu**L1**) (**1**) and ([Cu**L2**)(μ-ac)Cu(μ-ac)Cu**L2**) (**2**) of the tridentate aminosaccharide-derived Schiff-base ligands H_2**L1** [6-*N*-(salicylidene)amino-6-deoxy-1,2,3-tri-*O*-methyl-α-D-glucopyranoside] and H_2**L2** [6-*N*-(3,5-di-*tert*-butylsalicylidene)amino-6-deoxy-1,2,3-tri-*O*-methyl-α-D-glucopyranoside] were synthesized and structurally characterized. The trinuclear complex units can be described as two terminal copper–ligand moieties bridged by a central copper acetate moiety, with the Cu centers arranged in a triangular fashion. IR and UV/vis spectroscopic studies strongly indicate that the trinuclear structure is maintained in a methanolic solution. The temperature dependence of the magnetic susceptibility of both complexes shows a moderate antiferromagnetic coupling and can be well interpreted by applying a symmetric Cu_a–Cu_b–$Cu_{a'}$ model with linear spin topology. The fit of the magnetic data affords coupling constants J of –34 and –24 cm^{-1} for **1** and **2**, respectively [$\mathbf{H} = -J(\mathbf{S}_a\mathbf{S}_b + \mathbf{S}_b\mathbf{S}_{a'})$]. For μ-alkoxo-μ-acetato-bridged copper(II) complexes with a large dihedral angle between the adjacent coordination planes, as found in **1** and **2**, such an antiferromagnetic coupling is unusual. However, density functional theory calculations of **2** using BP86, B3LYP*, and B3LYP density functionals confirmed a symmetric doublet ground state.

Introduction

Much effort has been spent on the synthesis of mono-, bi-, and trinuclear copper complexes as functional and structural models of multicopper enzymes.[1−3] Apart from the biological significance, polynuclear metal complexes and complex assemblies are of great interest from the magnetochemical point of view.[4] Although the field of copper(II) complexes has been extensively studied with respect to binuclear systems,[5] only comparatively few examples of complexes containing more than two Cu centers have been reported. One approach for the synthesis of discrete polynuclear complexes is the introduction of compartmental ligands capable of holding together two or more metal ions.[6]

* To whom correspondence should be addressed: E-mail: sekr.plass@uni-jena.de.

† Institut für Anorganische und Analytische Chemie, Friedrich-Schiller-Universität Jena.

‡ Institut für Organische Chemie und Makromolekulare Chemie, Friedrich-Schiller-Universität Jena.

§ ETH Zürich.

¶ European Synchrotron Radiation Facility.

(1) Solomon, E. I.; Sundaram, U. M.; Machonkin, T. E. *Chem. Rev.* **1996**, *96*, 2563−2605.

(2) (a) Solomon, E. I.; Chen, P.; Metz, M.; Lee, S.-K.; Palmer, A. E. *Angew. Chem., Int. Ed.* **2001**, *40*, 4570−4590. (b) Pascaly, M.; Jolk, I.; Krebs, B. *Chem. Unserer Zeit* **1999**, *33*, 334−341. (c) Gerdemann, C.; Eicken, C.; Krebs, B. *Acc. Chem. Res.* **2002**, *35*, 183−191.

(3) (a) Reedijk, J.; Bouwman, E. *Bioinorganic Catalysis*; Marcel Dekker Inc.: New York, 1999. (b) Vigato, P. A.; Tamburini, S. *Coord. Chem. Rev.* **2004**, *248*, 1717−2128.

(4) (a) Kahn, O. *Acc. Chem. Res.* **2000**, *33*, 647−657. (b) Mrozinski, J. *Coord. Chem. Rev.* **2005**, *249*, 2534−2548.

(5) Kahn, O. *Molecular Magnetism*; VCH: Weinheim, Germany, 1993.

(6) (a) Tuna, F.; Patron, L.; Journaux, Y.; Andruh, M.; Plass, W.; Trombe, J.-C. *J. Chem. Soc., Dalton Trans.* **1999**, 539−545. (b) Chen, X.; Zhan, S.; Hu, C.; Meng, Q.; Liu, Y. *J. Chem. Soc., Dalton Trans.* **1997**, 245−250. (c) Paital, A. R.; Nanda, P. K.; Das, S.; Aromí, G.; Ray, D. *Inorg. Chem.* **2006**, *45*, 505−507.

10.1021/ic0605064 CCC: $33.50
Published on Web 11/14/2006

Another way toward polynuclear complexes is the use of bi- or tridentate terminal ligands[7] and multiatom bridging ligands such as carboxylato groups.[8] For trinuclear copper(II) complexes, the metal atoms are arranged in either a triangular[9,10] or a linear fashion,[11−13] with the latter case being less common. The predominant magnetic interaction between the metal centers in most of the known polynuclear copper(II) complexes is antiferromagnetic, which is in accordance with the antiferromagnetically coupled metal centers in the active sites of multicopper enzymes.[1] Whereas cases of a ferromagnetic interaction in polynuclear copper(II) complexes are comparatively rare (selected examples are reported in refs 10, 12, and 14).

Sugar-based ligands have been proven to be very useful as chiral auxiliaries, leading to an extensive search for new carbohydrate derivatives and their metal complexes,[15] which have been applied as catalysts in a great variety of reactions.[16] The advantage of using carbohydrate derivatives as ligands is that they are readily available and highly functionalized and provide several stereogenic centers. Introduction of hetero donor atoms[17] like N, S, and P and of entire functional groups[18] has opened a new field of coordination chemistry. As a consequence of their potential biological relevance and catalytic activity, copper(II) complexes of aminosugar-based ligands are of particular interest. Nevertheless, the number of such complexes is still limited, with some reported examples for ligands derived from condensation of aminocarbohydrates with 3-oxoenamines[19,20] or *o*-hydroxyaldehydes.[21] Herein we report the synthesis of two new trinuclear copper(II) complexes derived from Schiff-base ligands based on the aminosugar 6-amino-6-deoxy-1,2,3-tri-*O*-methyl-α-D-glucopyranoside along with their structural, magnetic, and spectroscopic characterization, revealing unusual properties.

Experimental Section

Materials. Chemicals and solvents were obtained from commercial sources and used without further purification if not stated otherwise. Methanol and ethanol were dried by distillation from an alcohol/sodium alcoholate mixture under argon. Thin-layer chromatography (TLC) was conducted on Merck glass plates coated with silica gel 60. Chromatography was performed using silica gel 60 (particle size 0.063−0.2 mm) from Fluka Chemie GmbH and sephadex LH-20 from Pharmacia Fine Chemicals AB.

Physical Measurements. NMR spectra were recorded at 250 MHz on a Bruker AC-200 spectrometer. IR spectra were measured on a Bruker Equinox 55 spectrometer. A HATR accessory from Pike was used for solution IR measurements, and the solution sample was layered on a ZnSe crystal. Solid-state samples were measured as KBr pellets. UV/vis solution spectra were recorded on a Cary 5000 from Varian. For the solid-state electronic spectra, the samples were diluted with barium sulfate. A Cary 5E from Varian with a diffuse-reflectance accessory "praying mantis" from Harrick was used for the solid-state measurements. Mass spectra were carried out on a Finnigan MAT SSQ710 or a Finnigan MAT 95XLTRAP. Elemental analyses were acquired by use of a Leco CHNS 932. Magnetic susceptibilities were measured on a MPMSR-5S−SQUID magnetometer from Quantum Design in the range from 2 to 300 K at magnetic fields of 2000 and 5000 Oe. Diamagnetic corrections were estimated according to Pascal's constants.

Synthesis of Compounds. The aminosaccharide 6-amino-6-deoxy-1,2,3-tri-*O*-methyl-α-D-glucopyranoside was obtained in a five-step synthesis by applying procedures reported in the literature.[22−26]

General Procedure for the Schiff-Base Ligands. A total of 4.5 mmol of salicylaldehyde or 3,5-di-*tert*-butylsalicylaldehyde was added to a solution of 4.5 mmol of 6-amino-6-deoxy-1,2,3-tri-*O*-methyl-α-D-glucopyranoside in 20 mL of dry ethanol and refluxed for 2 h until TLC showed completion (eluent: ethyl acetate/methanol 1:2). After removal of the solvent under reduced pressure, the crude product was dried in vacuo and purified by column chromatography using silica gel (eluent: ethyl acetate).

6-*N*-(Salicylidene)amino-6-deoxy-1,2,3-tri-*O*-methyl-α-D-glucopyranoside (H_2L1). Yield: 1.39 g (95%). Anal. Calcd for $C_{16}H_{23}NO_6$ (M = 325.36 g/mol): C, 59.06; H, 7.13; N, 4.31.

(7) Costa, R.; Garcia, A.; Ribas, J.; Mallah, T.; Journaux, Y.; Sletten, J.; Xolans, X.; Rodríguez, V. *Inorg. Chem.* **1993**, *32*, 3733−3742.
(8) Colacio, E.; Dominguez-Vera, J. M.; Moreno, J. M.; Riuz, J.; Kivekäs, R.; Romerosa, A. *Inorg. Chim. Acta* **1993**, *212*, 115−121.
(9) (a) Liu, X.; de Miranda, M. P.; McInnes, E. J. L.; Kilner, C. A.; Halcrow, M. A. *J. Chem. Soc., Dalton Trans.* **2004**, 59−64. (b) Bian, H.-D.; Gu, W.; Xu, J.-Y.; Bian, F.; Yan, S.-P.; Liao, D.-Z.; Jiang, Z.-H.; Cheng, P. *Inorg. Chem.* **2003**, *42*, 4265−4267. (c) Angaridis, P. A.; Baran, P.; Bocă, R. R.; Cervantes-Lee, F.; Haase, W.; Mezei, G.; Raptis, R. G.; Werner, R. *Inorg. Chem.* **2002**, *41*, 2219−2228.
(10) Mukhopadhyay, S.; Mandal, D.; Chatterje, P. B.; Desplanches, C.; Sutter, J.-P.; Butcher, R. J.; Chaudhury, M. *Inorg. Chem.* **2004**, *43*, 8501−8509.
(11) (a) van Albada, G. A.; Mutikainen, I.; Turpeinen, U.; Reedijk, J. *Eur. J. Inorg. Chem.* **1998**, 547−549. (b) Aghmiz, M.; Aghmiz, A.; Díaz, Y.; Masdeu-Bultó, A.; Claver, C.; Castillón, S. *J. Org. Chem.* **2004**, *69*, 7502−7510.
(12) Gutierrez, L.; Alzuet, G.; Real, J. A.; Cano, J.; Borrás, J.; Castiñeiras, A. *Inorg. Chem.* **2000**, *39*, 3608−3614.
(13) Song, Y.; Gamez, P.; Roubeau, O.; Mutikainen, I.; Turpeinen, U.; Reedijk, J. *Inorg. Chim. Acta* **2005**, *358*, 109−115.
(14) Haase, W.; Gehring, S. *J. Chem. Soc., Dalton Trans.* **1985**, 2609−2613.
(15) Alexeev, Y. E.; Vasilchenko, I. S.; Kharisov, B. I.; Blanco, L. M.; Garnovskii, A. D.; Zhdanov, Y. A. *J. Coord. Chem.* **2004**, *57*, 1447−1517.
(16) (a) Diéguez, M.; Pámies, O.; Ruiz, A.; Díaz, Y.; Castillón, S.; Claver, C. *Coord. Chem. Rev.* **2004**, *248*, 2165−2192. (b) Diéguez, M.; Pámies, O.; Claver, C. *Chem. Rev.* **2004**, *104*, 3189−3215.
(17) (a) Pámies, O.; Diéguez, M.; Net, G.; Ruiz, A.; Claver, C. *Organometallics* **2000**, *19*, 1488−1496. (b) Pámies, O.; Diéguez, M.; Net, G.; Ruiz, A.; Claver, C. *J. Org. Chem.* **2001**, *66*, 8364−8369. (c) Boog-Wick, K.; Pregosin, P. S.; Trabesinger, G. *Organometallics* **1998**, *17*, 3254−3264.
(18) (a) Ferrara, M. L.; Giordano, F.; Orabona, I.; Panunzi, A.; Ruffo, F. *Eur. J. Inorg. Chem.* **1999**, 1939−1947. (b) Fridgen, J.; Herrmann, W. A.; Eickerling, G.; Santos, A. M.; Kühn, F. E. *J. Organomet. Chem.* **2004**, *689*, 2752−2761. (c) Becher, J.; Seidel, I.; Plass, W.; Klemm, D. *Tetrahedron* **2006**, *62*, 5675−5681.
(19) Wegner, R.; Gottschaldt, M.; Görls, H.; Jäger, E.-G.; Klemm, D. *Angew. Chem., Int. Ed.* **2000**, *39*, 595−599.
(20) (a) Wegner, R.; Gottschaldt, M.; Görls, H.; Jäger, E.-G.; Klemm, D. *Chem.—Eur. J.* **2001**, *7*, 2143−2157. (b) Wegner, R.; Gottschaldt, M.; Poppitz, W.; Jäger, E.-G.; Klemm, D. *J. Mol. Catal. A: Chem.* **2003**, *201*, 93−118. (c) Gottschaldt, M.; Wegner, R.; Görls, H.; Klüfers, P.; Jäger, E.-G.; Klemm, D. *Carbohydr. Res.* **2004**, *339*, 1941−1952.
(21) (a) Yan, S.; Klemm, D. *Tetrahedron* **2002**, *58*, 10065−10071. (b) Rajsekhar, G.; Sah, A. K.; Rao, C. P.; Guionneau, P.; Bharathy, M.; GuruRow, T. N. *Dalton Trans.* **2003**, 3126−3135. (c) Sah, A. K.; Kato, M.; Tanase, T. *Chem. Commun.* **2005**, 675−677. (d) Sah, A. K.; Tanase, T.; Mikuriya, M. *Inorg. Chem.* **2006**, *45*, 2083−2092. (e) Burkhardt, A.; Buchholz, A.; Görls, H.; Plass, W. *Eur. J. Inorg. Chem.* **2006**, 3400−3406.
(22) Zeller, S. G.; D'Ambra, A. J.; Rice, M. J.; Gray, G. R. *Carbohydr. Res.* **1988**, *182*, 53−62.
(23) Fuller, T. S.; Stick, R. V. *Aust. J. Chem.* **1980**, *33*, 2509−2515.
(24) Jacobsen, S. *Acta Chem. Scand., Ser. B* **1984**, *38*, 157−164.
(25) Fürstner, A.; Baumgartner, J.; Jumbam, D. N. *J. Chem. Soc., Perkin Trans. 1* **1993**, *1*, 131−138.
(26) Ko, K.-Y.; Park, J.-Y. *Tetrahedron Lett.* **1997**, *38*, 407−410.

Found: C, 59.39; H, 7.07; N, 4.00. ^{1}H NMR ($CDCl_3$, 250 MHz, ppm): δ 3.14 (1H, dd, J = 9.2 and 3.5 Hz, C-2-H), 3.29 (3H, s, $-OCH_3$), 3.40 (3H, s, $-OCH_3$), 3.57 (3H, s, $-OCH_3$), 3.37−3.58 (m, 4H, C-3-H, C-5-H, C-6-H), 3.95 (1H, d, J = 12.7 Hz, C-4-H), 4.71 (1H, d, J = 3.5 Hz, C-1-H), 6.75−8.81 (m, 2H, Ar), 7.14−7.22 (m, 2H, Ar), 8.27 (1H, s, N=C−H). ^{13}C NMR ($CDCl_3$, 63 MHz, ppm): δ 55.17, 58.40, 61.25 (all $-OCH_3$), 60.41 (C-6), 69.96 (C-4), 71.29 (C-5), 81.95 (C-3), 82.99 (C-2), 97.27 (C-1), 117.09, 118.46, 118.74, 131.36, 132.32, 161.35 (all Ar), 166.79 (C=N).

6-*N*-(3,5-Di-*tert*-butylsalicylidene)amino-6-deoxy-1,2,3-tri-*O*-methyl-α-D-glucopyranoside (H_2L2). Yield: 1.87 g (95%). Anal. Calcd for $C_{24}H_{39}NO_6$ (M = 437.57 g/mol): C, 65.88; H, 8.98; N, 3.20. Found: C, 66.54; H, 9.06; N, 3.06. ^{1}H NMR ($CDCl_3$, 250 MHz, ppm): δ 1.23 (9H, s, ^{t}Bu), 1.35 (9H, s, ^{t}Bu), 3.17 (1H, dd, J = 9.4 und 3.5 Hz, C-2-H), 3.31 (3H, s, $-OCH_3$), 3.41 (3H, s, $-OCH_3$), 3.57 (3H, s, $-OCH_3$), 3.36−3.80 (4H, m, C-3-H, C-5-H, C-6-H), 3.65 (1H, d, J = 12.6 Hz, C-4-H), 4.73 (1H, d, J = 3.5 Hz, C-1-H), 7.01 (1H, d, Ar), 7.52 (1H, d, Ar), 8.30 (1H, s, N=C−H). ^{13}C NMR ($CDCl_3$, 63 MHz, ppm): δ 29.35, 31.48 (both $-C(CH_3)_3$), 34.09, 35.00 (both $-C(CH_3)_3$), 55.10, 58.36, 61.26 (all $-OCH_3$), 59.73 (C-6), 70.03 (C-4), 71.27 (C-5), 81.96 (C-3), 83.00 (C-2), 97.23 (C-1), 117.81, 125.91, 126.91, 136.67, 139.87, 158.18 (all Ar), 167.82 (C=N).

General Procedure for the Copper Complexes. A methanolic solution of 1.5 equiv of anhydrous copper(II) acetate was reacted with a solution of 1 equiv of the Schiff-base ligand and 2 equiv of triethylamine in 25 mL of dry methanol. The solution color turns immediately from yellow to dark green upon the addition of the copper(II) salt. After stirring for about 1 h at room temperature, the solvent was removed under reduced pressure, and the remaining crude product was dried in vacuo and purified by column chromatography using sephadex LH-20 (eluent: methanol). Single crystals suitable for X-ray diffraction were obtained from a methanolic solution by slow evaporation. Microcrystalline samples for the SQUID measurements and spectroscopic studies were obtained by fast evaporation.

Bis(μ-acetato)bis[6-*N*-(salicylidene)amino-6-deoxy-1,2,3-tri-*O*-methyl-α-D-glucopyranosido]tricopper(II) (1). Two crystalline modifications were obtained for complex **1**. Applying the general procedure led to modification **1a**. Modification **1b** was obtained by using copper(II) acetate monohydrate (instead of the anhydrous salt) and technical-grade methanol. Single crystals suitable for X-ray crystallography could be obtained directly from the reaction solution. Significant electron density remained after processing of the structure solution, indicating the presence of a number of strongly disordered solvent molecules, mostly located at partially occupied crystallographic positions. Therefore, the remaining electron density was assigned to water and methanol molecules as appropriate. Elemental analysis of **1b** indicates the presence of four methanol molecules per complex unit. Microcrystalline samples of **1b** were used for all physical and spectroscopic measurements. Anal. Calcd for $C_{40}H_{64}N_2O_{20}Cu_3$ (**1**·4CH_3OH, M = 1083.58): C, 44.34; H, 5.95; N, 2.59. Found: C, 44.22; H, 5.28; N, 2.60. IR (KBr, cm^{-1}): 3448 br, 2931 w, 2909 w, 2837 w, 1622 s (C=N), 1554 s (COO), 1535 m, 1469 m, 1443 s, 1357 w, 1332 w, 1199 m, 1151 m, 1084 s, 1048 w, 961 w, 915 w, 763 w, 677 w. IR (MeOH, cm^{-1}): 2906 w, 2846 w, 1623 s (C=N), 1559 s (COO), 1540 m, 1472 w, 1437 s, 1200 m, 1154 m, 1085 s, 962 m. UV/vis (MeOH): λ_{max} (ϵ, L mol^{-1} cm^{-1}) 665 (340), 368 (11 700), 269 (32 600), 239 (49 400), 223 (54 600) nm. UV/vis ($BaSO_4$): λ_{max} 677, 372, 273, 243, 228 (sh) nm. MS (ESI in MeOH): m/z 1183 (18%) [Cu_3(**L1**)$_3$ + Na]$^+$, 796 (39%) [Cu_2(**L1**)$_2$ + Na]$^+$, 774 (100%) [Cu_2(**L1**)$_2$ + H]$^+$, 409 (20%) [Cu(**L1**) + Na]$^+$, 387 (8%) [Cu(**L1**) + H]$^+$.

Bis(μ-acetato)bis[6-*N*-(3,5-Di-*tert*-butylsalicylidene)amino-6-deoxy-1,2,3-tri-*O*-methyl-α-D-glucopyranosido]tricopper(II) (2). Anal. Calcd for $C_{52}H_{80}N_2O_{16}Cu_3$ (M = 1179.83): C, 52.94; H, 6.83; N, 2.37. Found: C, 53.08; H, 6.92; N, 2.12. IR (KBr, cm^{-1}): 2953 s, 2908 s, 1617 s (C=N), 1559 s (COO), 1534 m, 1433 s, 1363 w, 1336 w, 1257 w, 1200 w, 1171 m, 1087 s, 953 w, 841 w, 790 w, 747 w, 678 w. IR (MeOH, cm^{-1}): 2960 w, 1616 m (C=N), 1559 m (COO), 1436 w, 1258 w, 1172 w, 1083 m, 959 w. UV/vis (MeOH): λ_{max} (ϵ, L mol^{-1} cm^{-1}) 661 (410), 385 (11 800), 276 (32 000), 246 (42 900) (sh), 230 (52 800) nm. UV/vis ($BaSO_4$): λ_{max} 658, 403, 281, 252 (sh), 232 nm. MS (ESI in MeOH): m/z 1519 (37%) [Cu_3(**L2**)$_3$ + Na]$^+$, 1497 (28%) [Cu_3(**L2**)$_3$ + H]$^+$, 1020 (75%) [Cu_2(**L2**)$_2$ + Na]$^+$, 998 (100%) [Cu_2(**L2**)$_2$ + H]$^+$, 522 (10%) [Cu(**L2**) + Na]$^+$, 500 (20%) [Cu(**L2**) + H]$^+$.

X-ray Crystallographic Studies. The intensity data for the compounds **1a** and **1b** were collected on a Nonius Kappa CCD diffractometer, using graphite-monochromated Mo Kα radiation. Because for compound **2** the crystal size was insufficient for measurement utilizing low-intensity X-ray sources, the data collection was carried out at the ESRF at beamline ID11 using a Bruker Smart CCD camera system at fixed 2θ, while the sample was rotated over 0.1° intervals during 2-s exposures, using monochromated radiation from λ = 0.509 15 Å. Data were corrected for Lorentz and polarization effects but not for absorption.[27] Details of the data collection and refinement procedure are summarized in Table 1. All structures were solved by direct methods with the program *SHELXS-97*[28] and refined by full-matrix least-squares techniques against F_o^2 with the software package *SHELXL-97*.[28] All non-hydrogen atoms were refined anisotropically, except oxygen atoms of the water molecules in **1b**. Because of the quality of the crystals of compound **2**, several peaks of residual electron density could be located in the final Fourier map near the copper atoms. Attempts to solve the structure for a data set with additional absorption correction have been unsuccessful in leading to any improvement, as have been attempts of twin refinement. The program *XP* (Siemens Analytical X-ray Instruments, Inc.) was used for structure representations.

Crystallographic data (excluding structure factors) have been deposited with the Cambridge Crystallographic Data Centre as supplementary publications CCDC-287127 for **1a**, CCDC-287128 for **1b**, and CCDC-602313 for **2**. Copies of the data can be obtained free of charge on application to CCDC, 12 Union Road, Cambridge CB2 1EZ, U.K., at www.ccdc.cam.ac.uk/conts/retrieving.html or deposit@ccdc.cam.ac.uk.

Quantum Chemical Methodology. *All-electron* calculations and geometry optimizations were performed with the quantum chemical program package *TURBOMOLE*.[29] Three density functionals, BP86[30] in combination with the resolution-of-the-identity (RI)

(27) (a) *SMART COLLECT*; Data Collection Software; Nonius BV: Delft, The Netherlands, 1998. (b) Otwinowski, Z.; Minor, W. Processing of X-ray Diffraction Data Collected in Oscillation Mode. In *Macromolecular Crystallography*; Carter, C. W., Jr., Sweet, R. M., Eds.; Methods in Enzymology, Vol. 276, Part A; Academic Press: New York, 1997; pp 307−326.
(28) Sheldrick, G. M. *SHELXS97 and SHELXL97*; University of Göttingen: Göttingen, Germany, 1997.
(29) *TURBOMOLE*, http://www.cosmologic.de/QuantumChemistry/main_turbomole.html.
(30) (a) Becke, A. D. *Phys. Rev. A* **1988**, *38*, 3098−3100. (b) Perdew, J. P. *Phys. Rev. B* **1986**, *33*, 8822−8824.

Table 1. Crystal Data, Data Collection, and Refinement Parameters for Compounds **1a**, **1b**, and **2**

	1a	**1b**	**2**
formula	$C_{38.5}H_{59}N_2O_{19}Cu_3$	$C_{37.5}H_{67}N_2O_{24}Cu_3$	$C_{52}H_{80}N_2O_{16}Cu_3$
fw (g mol^{-1})	1044.50	1120.55	1179.80
T (K)	183(2)	183(2)	120(2)
cryst size (mm^3)	0.03 × 0.03 × 0.02	0.04 × 0.03 × 0.03	0.04 × 0.02 × 0.01
cryst syst	triclinic	triclinic	monoclinic
space group	$P1$	$P1$	$P2_1$
a (Å)	9.6351(7)	11.4800(3)	12.3922(6)
b (Å)	10.9631(8)	21.9824(4)	13.6352(5)
c (Å)	12.0979(9)	22.2332(5)	17.2373(8)
α (deg)	91.097(5)	104.147(1)	90.000
β (deg)	113.140(4)	104.936(1)	97.978(2)
γ (deg)	101.633(5)	100.198(1)	90.000
V (Å^3)	1144.1(2)	5081.3(18)	2884.4(2)
Z	1	4	2
ρ_{calcd} (g cm^{-3})	1.516	1.465	1.358
radiation	Mo Kα	Mo Kα	synchrotron (λ = 0.509 15 nm)
μ (mm^{-1})	1.458	1.325	0.616
θ_{min}, θ_{max} (deg)	1.91, 27.54	1.92, 27.46	1.36, 20.71
unique data	8195	35629	12329
data with $I > 2\sigma(I)$	6997	26139	9931
no. of param	591	2325	672
wR2[a] (all data, F_o^2)	0.105	0.153	0.294
R1[b] [$I > 2\sigma(I)$]	0.043	0.057	0.100
Flack param	−0.008(12)	0.016(9)	0.07(4)

[a] wR2 = $[\sum w(F_o^2 - F_c^2)^2/\sum w(F_o^2)^2]^{1/2}$ with $w^{-1} = \sigma^2(F_o^2) + (xP)^2 + yP$ and $P = (1/3)[\max(0,F_o^2) + 2F_c^2]$. [b] R1 = $\sum||F_o| - |F_c||/ - |F_o|$.

Scheme 1

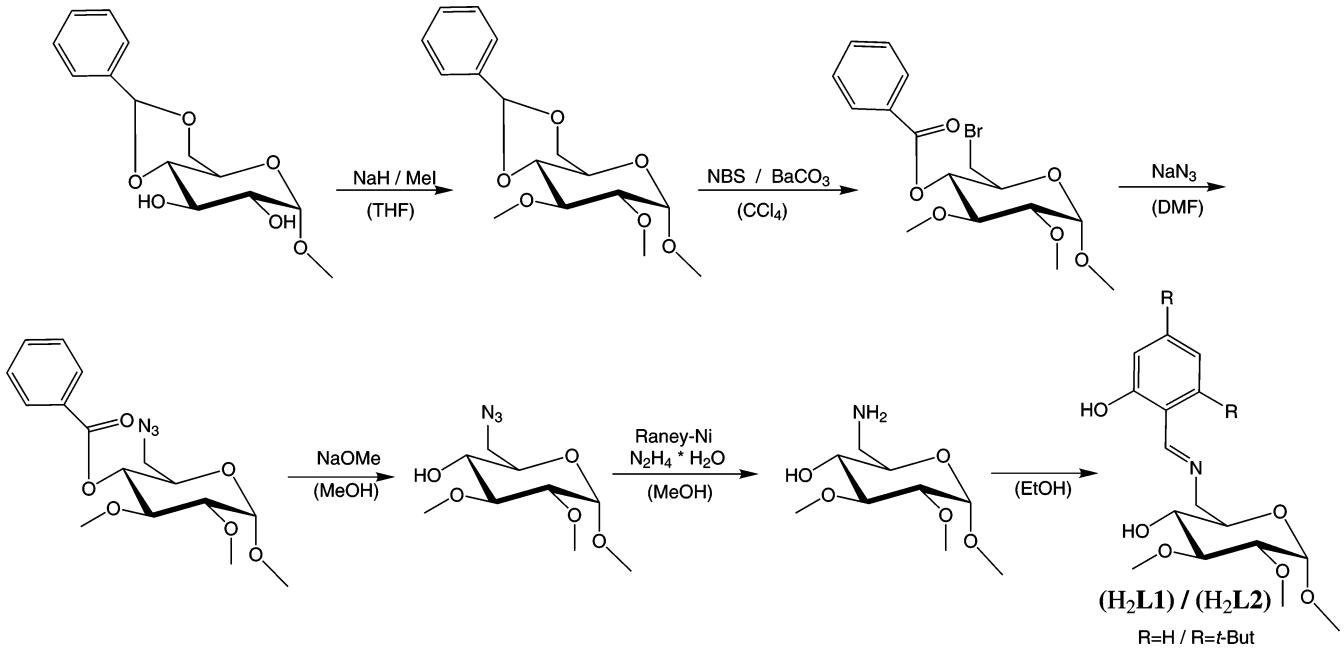

density-fitting technique,[31,32] B3LYP,[33] and B3LYP*,[34,35] were employed. The B3LYP* functional is a modification of the well-known B3LYP functional, where the exact exchange admixture is set to 15% (instead of 20% as in B3LYP). For B3LYP* calculations, a modified implementation of *TURBOMOLE*'s DSCF module was used. We employed the TZVP basis by Schäfer et al.[36] throughout, featuring a valence triple-ζ basis set with polarization functions on all atoms. For calculation of local spin expectation values, our implementation described in ref 37 in *TURBOMOLE* was applied, which is based on work by Clark and Davidson.[38,39] Modified

(31) (a) Baerends, E. J.; Ellis, D. E.; Ros, P. *Chem. Phys.* **1973**, *2*, 41−51. (b) Dunlap, B. I.; Connolly, J. W. D.; Sabin, J. R. *J. Chem. Phys.* **1979**, *71*, 3396−3402.
(32) ftp://ftp.chemie.uni-karlsruhe.de/pub/jbasen.
(33) (a) Becke, A. D. *J. Chem. Phys.* **1993**, *98*, 5648−5652. (b) Stephens, P. J.; Devlin, F. J.; Chabalowski, C. F.; Frisch, M. J. *J. Phys. Chem.* **1994**, *98*, 11623−11627.
(34) (a) Reiher, M. *Inorg. Chem.* **2002**, *41*, 6928−6935. (b) Reiher, M.; Salomon, O.; Hess, B. A. *Theor. Chem. Acc.* **2001**, *107*, 48−55.
(35) Salomon, O.; Reiher, M.; Hess, B. A. *J. Chem. Phys.* **2002**, *117*, 4729−4737.
(36) ftp://ftp.chemie.uni-karlsruhe.de/pub/basen.
(37) Herrmann, C.; Reiher, M.; Hess, B. A. *J. Chem. Phys.* **2005**, *122*, 034102.
(38) (a) Davidson, E. R.; Clark, A. E. *Mol. Phys.* **2002**, *100*, 373−383. (b) Clark, A. E.; Davidson, E. R. *J. Chem. Phys. A* **2002**, *106*, 6890−6896. (c) O'Brien, T. A.; Davidson, E. R. *Int. J. Quantum Chem.* **2003**, *92*, 294−325.
(39) Clark, A. E.; Davidson, E. R. *J. Chem. Phys.* **2001**, *115*, 7382−7392.

Löwdin projectors,[39,40] denoted by Löwdin*, were used for the local decomposition, which differ from the "standard" Löwdin projectors by an orthogonalization of the basis set within atomic centers prior to the Löwdin orthogonalization. Frequency calculations for the prediction of the IR spectrum of **2** were carried out with the SNF package.[41]

Results and Discussion

Synthesis. 6-Amino-6-deoxy-1,2,3-tri-*O*-methyl-α-D-glucopyranoside was synthesized according to published procedures as outlined in Scheme 1 starting from methyl-4,6-*O*-benzylidene-α-D-glucopyranoside. Deprotonation with sodium hydride followed by methylation with methyl iodide[22] and nucleophilic ring-opening reaction of the benzylidene acetal with *N*-bromosuccinimide[23] gave 6-bromo-6-deoxy-4-*O*-benzoyl-1,2,3-tri-*O*-methyl-α-D-glucopyranoside. By substitution of the bromide with NaN_3,[24] cleavage of the benzoyl ester,[25] and reduction of the azide with Raney nickel/hydrazine hydrate,[26] the aminosaccharide could be obtained. The Schiff-base ligands H_2**L1** and H_2**L2** were synthesized by the reaction of equimolar amounts of 6-amino-6-deoxy-1,2,3-tri-*O*-methyl-α-D-glucopyranoside and the corresponding salicylaldehyde derivative in dry ethanol.

The copper(II) complexes [Cu(**L1**)(μ-ac)Cu(μ-ac)Cu(**L1**)] (**1**) and [Cu(**L2**)(μ-ac)Cu(μ-ac)Cu(**L2**)] (**2**) were prepared by adding a methanolic solution of 1.5 equiv of copper(II) acetate to a methanolic solution of the ligand and 2 equiv of triethylamine at room temperature. The color of the reaction mixture turns immediately from yellow to dark green (blue-green in the case of **1**). Single crystals suitable for crystal structure analysis were obtained by slow evaporation of the solvent after a few days.

Crystal Structures. The molecular structure of **1** is illustrated in Figure 1. The molecular structure of complex **2** shows very similar features and is presented in Figure S1 in the Supporting Information. Selected atomic distances are given in Table 2 for both complexes, whereas selected angles are summarized in Tables S1 and S2 in the Supporting Information. **1** crystallizes in two modifications (both in space group *P*1), depending on the content of water in the reaction solvent. Apart from the content of solvent molecules, the structural features of the complex moieties in the modifications **1a** and **1b** differ very little (see the Supporting Information), so that in this paper, only the data set obtained for **1a** is used to discuss the molecular structure of **1**.

Both complexes, **1** and **2**, show a folded trinuclear structure comprising three copper(II) ions, two dianionic ligand molecules (with the hydroxy group of the sugar moiety and the phenolic OH group being deprotonated upon coordination), and two acetate ions. The terminal copper centers (Cu1 and Cu2) in each structure are coordinated by a ligand molecule (**L1** or **L2**) and bridged to the central copper atom by two acetate ions and the deprotonated saccharide hydroxy group. Overall, the arrangement can be described as two terminal copper−ligand fragments and one central bridging copper acetate fragment.

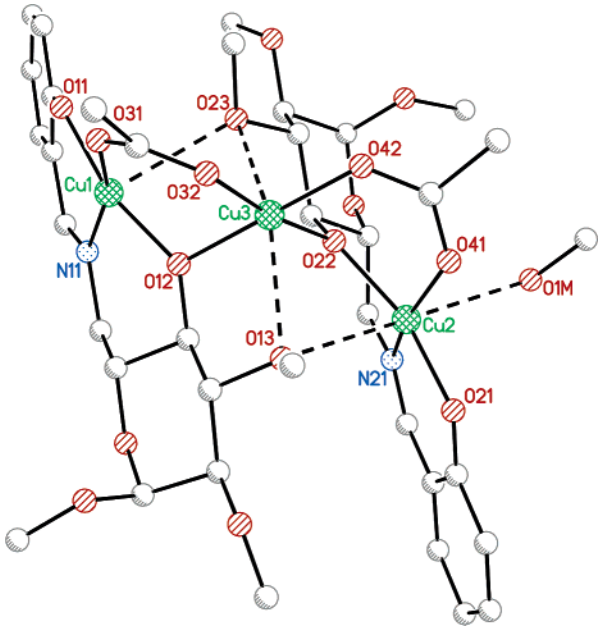

Figure 1. Molecular structure of **1**. Bonds to weakly bound axial donor atoms are given as dashed lines. Hydrogen atoms and noncoordinated solvent molecules are omitted for clarity.

Table 2. Selected Atomic Distances (Å) for **1** (in Crystals of **1a**) and **2**

	1	**2**		**1**	**2**
Cu1−O11	1.883(4)	1.850(7)	Cu2−O1M	2.634(1)	
Cu1−O12	1.896(4)	1.889(6)	Cu3−O12	1.945(4)	1.954(7)
Cu1−O23	2.670(1)	2.861(1)	Cu3−O13	2.518(1)	2.579(1)
Cu1−O31	1.963(4)	1.957(9)	Cu3−O22	1.932(4)	1.942(7)
Cu1−N11	1.953(4)	1.939(10)	Cu3−O23	2.610(1)	2.570(1)
Cu2−O21	1.917(4)	1.870(7)	Cu3−O32	1.945(4)	1.939(8)
Cu2−O22	1.924(4)	1.904(6)	Cu3−O42	1.948(4)	1.950(8)
Cu2−O13	2.830(1)	2.511(1)	Cu1···Cu2	5.7426(9)	5.6048(17)
Cu2−O41	1.984(4)	1.975(10)	Cu1···Cu3	3.1855(9)	3.1952(17)
Cu2−N21	1.956(4)	1.965(9)	Cu2···Cu3	3.2262(8)	3.1691(16)

The coordination environments of the terminal copper centers in each structure are very similar and differ just slightly in bond distances (Table 2) and angles (Table S1 and S2 in the Supporting Information). The two terminal copper centers Cu1 and Cu2 possess a distorted square-planar arrangement, with the largest deviation observed at Cu2 in **2** with a trans-bonding angle O41−Cu2−N21 of 148.5°. The square-pyramidal [O_4N] coordination spheres of Cu1 and Cu2 are completed by the weakly bound methyl ether oxygen atoms O23 and O13, respectively, which belong to the opposite copper−ligand moiety. The Cu2 atom in **1** is additionally coordinated by one methanol molecule (O1M) occupying the second axial position, leading to a distorted octahedral [O_5N] coordination. The central copper atom Cu3 is coordinated by the sugar oxygen donor atoms O12 and O22 as well as the oxygen atoms O32 and O42 of the bridging acetate ions, leading to an almost ideal square-planar arrangement of the equatorial coordination plane (displacement of copper atoms from the mean planes is 0.015 Å for **1** and 0.003 Å for **2**). The overall distorted octahedral [O_6] coordination sphere with elongated axial bonds is completed by the weakly bound methyl ether oxygen atoms O13 and

(40) Löwdin, P.-O. *J. Chem. Phys.* **1950**, *18*, 365−375.
(41) Neugebauer J.; Reiher, M.; Kind, C.; Hess, B. A. *J. Comput. Chem.* **2002**, *23*, 895−910; www.theochem.ethz.ch/software/snf.

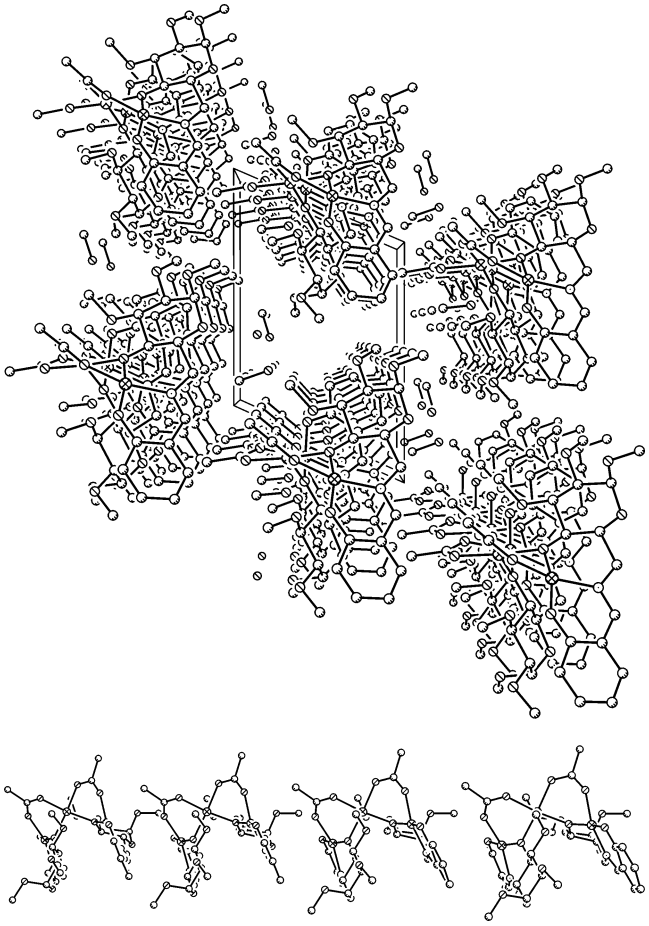

Figure 2. Top: Supramolecular arrangement of complex **1** in the crystal structure of **1a** (view along the crystallographic *b* axis). Bottom: One-dimensional stacking of **1** with the equatorial coordination planes of the terminal copper atoms of adjacent complex units oriented in a coplanar fashion.

O23, functioning as an additional axial bridge between the metal centers.

This leads to a characteristic deviation from the linear arrangement of the trinuclear complexes, which is best described as a V-like folding of the terminal copper−ligand moieties (Cu1 and Cu2) representing the "wings", which are connected through the central copper atom Cu3, as illustrated for complex **1** in Figure S2 in the Supporting Information. As a consequence, the equatorial coordination planes of the terminal copper atoms are almost coplanar with the angles of 4° for **1** and 7° for **2** and the Cu1−Cu3−Cu2 angles were found to be 127° (**1**) and 123° (**2**). The dihedral angles between the square-planar coordination mean plane of the central copper atom Cu3 and the equatorial coordination mean planes of the terminal copper atoms Cu1 and Cu2 are 66° and 69° for **1** as well as 63° and 68° for **2**, respectively.

The supramolecular arrangement of the trinuclear complex units in the crystal lattice exhibits distinct differences as the modifications of **1** and **2** are compared. For the modifications of **1**, the complex moieties are stacked in one-dimensional rows, with the "wings" of the V-shaped units oriented in a roughly parallel fashion. This is illustrated for the case of **1a** in Figure 2. The intermolecular Cu−Cu distance between the terminal metal centers of two adjacent complex units is 5.550 Å. Solvent molecules (methanol and water) are positioned in the space between the complex rows and assemble a hydrogen-bonding network. In **2**, no comparable stacking pattern is observed in the crystal structure. The sterically demanding *tert*-butyl groups fill the intermolecular space and provide a rather hydrophobic environment, and no solvent molecules are incorporated in the crystal lattice. The closest intermolecular Cu−Cu distances in **2** are 7.441 and 8.260 Å.

Table 3. Comparison of the Absorption Bands (λ in nm) in Electronic Spectra of the Complexes **1** (modification **1b**) and **2** in a Methanol Solution and the Solid State (in Parentheses)

1	**2**	**1**	**2**
223 (228)	230 (232)	368 (372)	385 (403)
239 (243)	246 (252)	665 (677)	661 (658)
269 (273)	276 (281)		

Spectroscopic Studies. From the copper acetato bridged solid-state structure of both complexes, the question arises as to whether this trimeric moiety is also maintained in solution. Electrospray ionization (ESI) mass spectra of **1** (modification **1b**) and **2** showed no evidence for the existence of the [CuL(μ-ac)Cu(μ-ac)CuL] trimers in a methanolic solution; only signals caused by CuL adducts of varying stoichiometry could be observed. To verify whether the complex trimers still exist in a methanolic solution and simply decompose under the experimental conditions in the mass spectrometer or really undergo solvolysis in methanol, electronic and vibrational spectroscopic measurements were carried out in the solid state as well as in a methanolic solution. A comparison of the resulting data should provide insight into the chemical composition of the complexes in solution. For all spectroscopic studies of complex **1**, samples of modification **1b** were used.

The data of the electronic spectra are given in Table 3. An assignment of the absorption bands is difficult because of the presence of two distinct chromophors. The absorption spectra of the methanolic solutions of **1** and **2** are very similar, but in the case of complex **2**, the absorption bands (except the weak transition in the visible range) are slightly red-shifted by 7−17 nm. This effect can be ascribed to the presence of the electron-pushing *tert*-butyl groups in **2**. Both compounds show a very broad d−d transition band around 665 nm (**1**) and 661 nm (**2**). The stronger absorption bands at 368 nm (**1**) and 385 nm (**2**) can be ascribed to a charge-transfer transition from the phenolate moieties to the terminal copper ions.

The diffuse-reflectance spectra (see Table 3) reveal high similarities to the corresponding solution data, even though the bands are much broader and the signal maxima, therefore, less precisely defined. The d−d transition bands appear around 677 nm (**1**) and 658 nm (**2**), which is in good agreement with the values of the solution spectra (665 and 661 nm, respectively). The charge-transfer transitions are found around 372 nm for **1** and 403 nm for **2**, compared to 368 and 385 nm, respectively, in solution. In contrast with the ESI mass spectra, these similarities suggest that the trimeric structure of the complexes found in the solid state could be maintained in a methanolic solution.

A spectroscopic feature that is more characteristic for the bridging copper acetate unit and thus more significant with respect to the question of the stability of the trimeric structure in solution is the vibrational band of the acetate bridge. IR spectroscopic studies on crystalline samples as KBr pellets of both complexes show broad absorption bands at 1554 cm^{-1} for **1** and 1559 cm^{-1} for **2** (with shoulders at 1535 and 1534 cm^{-1}, respectively), which are absent in the spectra of the pure ligands and can be assigned to the bridging acetate ions. The corresponding solution spectra (in methanol) differ only very slightly from the solid-state spectra, and most importantly the vibrational band of the acetate ion is still present at 1559 cm^{-1} for both complexes **1** and **2** with relatively large intensity. To verify that the observed vibrations are characteristic for the *bridging* acetate ions and not simply caused by free copper acetate upon dissociation of the trimeric complex moieties, control measurements were carried out with methanolic solutions of copper acetate and sodium acetate under the same conditions. In both cases, the observed vibrational bands (1627 cm^{-1} for copper acetate and 1580 cm^{-1} for sodium acetate; both values are constant in the examined concentration range) differ significantly from the values obtained for **1** and **2**. In addition, only trace amounts of free acetic acid (1708 cm^{-1}) could be detected in the methanolic solutions of **1** and **2**, which is clearly different from the solution spectra of sodium and copper acetate, where this band exhibits a significant intensity at comparable salt concentrations.

Finally, the predicted vibrational spectrum for **2** features two bands at 1522 and 1536 cm^{-1}, which are due to coupled vibrations of both bridging acetate ligands (harmonic BP86/RI/TZVP force field). These two vibrations possess significant IR intensities, with the mode at 1522 cm^{-1} showing the strongest absorption of all of the modes in the calculation, and do not couple notably with any other vibrations in the molecule (see Figure S3 in the Supporting Information). Moreover, these two vibrations are quite isolated in that wavenumber range, especially from the higher wavenumber region, with the next vibration found at 1593 and 1594 cm^{-1} (relative intensities 0.85 and 0.05), which are related to the coupled stretching vibrations of the two C═N bonds of the coordinating Schiff-base ligands. The situation is somewhat different on the low-energy end because two rather closely spaced bands at 1515 and 1517 cm^{-1} are predicted (relative intensities are about 0.2), which are related to aromatic C═C stretching vibrations. Nevertheless, the overall separation of this group of bands from the lower wavenumber region is significant, with bands starting at 1486 cm^{-1} showing only very low relative intensities (smaller than 0.05). Therefore, the discussed spectroscopic studies strongly indicate that the trimeric structure of the complexes **1** and **2** is retained in a methanolic solution.

Magnetochemistry. The magnetic properties of the trinuclear copper(II) complexes **1** (modification **1b**) and **2** were determined by magnetic susceptibility measurements of microcrystalline samples with a SQUID magnetometer as a function of temperature in the range from 2 to 300 K. The χ_M and $\chi_M T$ plots of the obtained data are given in Figures 3 and 4. The magnetic behavior of both complexes is quite similar, as could be expected considering the similarity in their molecular structures. At room temperature, both compounds show a paramagnetic behavior with $\chi_M T$ values of 1.35 cm^3 K mol^{-1} for **1** and 1.22 cm^3 K mol^{-1} for **2**, which is in good agreement with the theoretical spin-only value for three independent $S = {}^1/_2$ centers per molecule.[5] At temperatures below 100 K, both complexes show an antiferromagnetic coupling of the copper centers, leading to a decrease of the $\chi_M T$ values. In the case of **2**, the slope of the curve is decreasing toward very low temperatures, indicating a plateau at $\chi_M T = 0.44$ cm^3 K mol^{-1} for 2 K. In this temperature range, the $\chi_M T$ curve of complex **1** differs slightly from the one of complex **2**. The curve is not bending toward a plateau as smoothly as in the case of **2**; instead, a very small shoulder between 2 and 10 K with a $\chi_M T$ value of about 0.5 cm^3 K mol^{-1} is observed. The low-temperature data of both complexes are in agreement with the spin-only value for a $S = {}^1/_2$ system.[5] Therefore, both complexes are best described as paramagnetic systems with three independent copper(II) centers at high temperatures, whereas at very

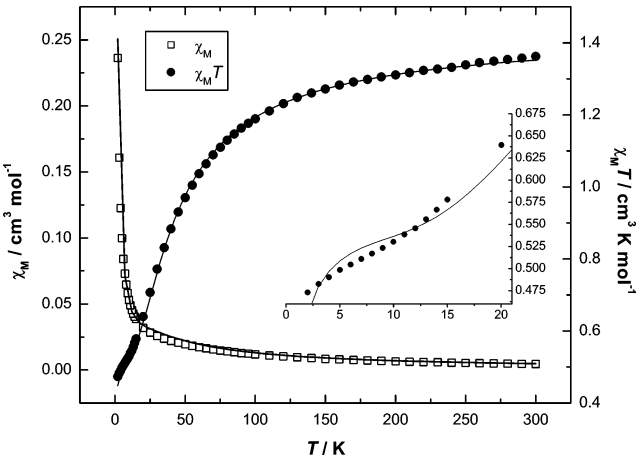

Figure 3. Plot of χ_M and $\chi_M T$ vs T for complex **1** at an applied field of 2000 Oe. The corresponding fit functions are drawn as solid lines (for parameters, see the text). The inset shows the $\chi_M T$ values between 2 and 20 K.

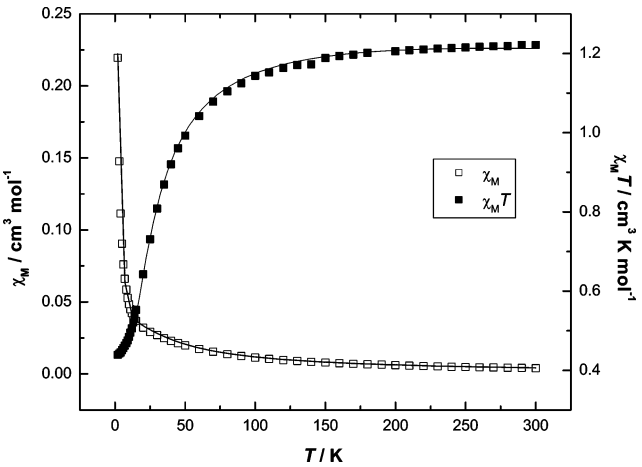

Figure 4. Plot of χ_M and $\chi_M T$ vs T for complex **2** at an applied field of 2000 Oe. The corresponding fit functions are drawn as solid lines (for parameters, see the text).

low temperatures, the system is antiferromagnetically coupled with a doublet ground state.

The coordination compounds **1** and **2** can be considered as approximately symmetric trinuclear $Cu_a-Cu_b-Cu_{a'}$ species. Slight differences in the bond distances and angles between the terminal copper centers as well as the weakly coordinated additional axial methanol ligand in **1** should not significantly effect the coupling of the magnetic orbitals. The energies of the low-lying states of such a system are obtained by using the isotropic spin Hamiltonian given in eq 1.

$$\mathbf{H} = -J(\mathbf{S}_{Cu_a}\mathbf{S}_{Cu_b} + \mathbf{S}_{Cu_b}\mathbf{S}_{Cu_{a'}}) - j\mathbf{S}_{Cu_a}\mathbf{S}_{Cu_{a'}} + g_{Cu_a}\beta H(\mathbf{S}_{Cu_a} + \mathbf{S}_{Cu_{a'}}) + g_{Cu_b}\beta H\mathbf{S}_{Cu_b} \quad (1)$$

Application of the Van Vleck equation and assuming identical average g values then lead to the theoretical expression for the magnetic susceptibility given in eq 2.[5]

$$\chi_M T = \frac{N\beta^2 g^2}{4k}\frac{1 + \exp[(J-j)/kT] + 10\exp[3J/2kT]}{1 + \exp[(J-j)/kT] + 2\exp[3J/2kT]} + (\mathrm{TIP})T \quad (2)$$

To obtain the magnetic coupling constants, the susceptibility data for complex **2** were fitted to eq 2. Attempts to determine the coupling constant j (corresponding to the interaction between the terminal copper centers) failed because of a strong dependence between the fit parameters j and J. Hence, this interaction was assumed to be negligible and j set to zero. Despite the triangular arrangement of the copper centers, both complexes exhibit, therefore, a linear spin topology from the magnetochemical point of view.

For complex **2**, the best fit of χ_M as well as of $\chi_M T$ as a function of temperature resulted in $J = -24(1)$ cm^{-1}, $g = 2.17(1)$, and a temperature-independent paramagnetism (TIP) of -2.2×10^{-4} cm^3 mol^{-1} with a coefficient of determination of $r^2 = 0.9987$.

In the case of **1**, the situation is more complicated. The $\chi_M T$ curve of **1** is not reaching a plateau at very low temperatures, as in the case of complex **2**; instead, it shows a very slight shoulder and a further decrease upon lowering of the temperature. To account for this behavior, weak intermolecular antiferromagnetic interactions between neighboring trinuclear units have to be included. The presence (in **1**) and absence (in **2**) of such interactions are in agreement with the different supramolecular arrangement of the complex units in the crystal lattice of both compounds. Moreover, intermolecular coupling in **1** might be supported by the hydrogen-bonding network of water and methanol molecules in the crystal.[13,42] According to the method of Ginsberg and Lines, the spin Hamiltonian in eq 1 is extended by the term $-zJ'\mathbf{S}_z\langle\mathbf{S}_z\rangle$ to take intermolecular exchange interactions into account.[43] The resulting parameters of the best fit for **1** are $J = -34(1)$ cm^{-1}, $g = 2.15(1)$, $zJ' = -0.73(9)$ cm^{-1}, and TIP $= 0.13(1)$ cm^3 mol^{-1} with a coefficient of determination of $r^2 = 0.9995$ (for details, see the Supporting Information).

The field dependence of the magnetization at 2 K shows saturation behavior (Figures S3 and S4 in the Supporting Information) and is in good agreement with the theoretical magnetization curve for an $S = {}^1/_2$ system, expressed by the Brillouin function[5] using the fitted g values. The magnetic saturation behavior of both complexes therefore confirms the doublet ground state at low temperatures, which was concluded from the temperature dependence of the magnetic susceptibility.

A lot of theoretical work has been spent on the interpretation of the magnetostructural correlations in di-μ-hydroxo- and di-μ-alkoxo-bridged copper(II) complexes,[44] and the linear dependence between the Cu−O−Cu bridging angle and the magnetic coupling constant is now well understood. In mixed-bridged complexes, the contribution of two different kinds of bridging units has to be taken into account and the situation gets more complicated. The two bridges may either add or counterbalance their effects, referred to as orbital complementarity and countercomplementarity.[45,46] This phenomenon has been explained in a number of studies by a two-step perturbation process.[47] In the first step, the symmetric ϕ_S and antisymmetric ϕ_{AS} combinations of the magnetic orbitals overlap with the symmetry-adapted highest occupied molecular orbital (HOMO) of one bridging unit to form new symmetric ϕ'_S and antisymmetric ϕ'_{AS} combinations, which are then combined with the HOMO of the second bridge, resulting in symmetric ϕ''_S and antisymmetric ϕ''_{AS} singly occupied molecular orbitals (SOMOs) of the dimeric complex unit. The second-step overlap can favor either the same (orbital complementarity) or the opposite (orbital countercomplementarity) combination of the first-step overlap, depending on structural parameters and the type of the bridging unit. The magnitude of the antiferromagnetic exchange coupling J_{AF} can be estimated from the energy gap $\Delta\epsilon$ between the SOMOs, according to $J_{AF} \sim (\Delta\epsilon)^2$.[48]

In the case of the present complexes **1** and **2**, the magnetic centers are bridged by an alkoxo unit and a carboxylato unit. To explain the magnetostructural correlations in a series of trinuclear μ-alkoxo-μ-carboxylato copper complexes, Gehring et al. compared experimental data and self-consistent-field chemical ionization calculations (on dimeric models) and found that the folding of the adjacent coordination planes is a decisive structural parameter for the exchange coupling.[49] Coplanarity (dihedral angle $\tau = 0°$) results in a large energy gap $\Delta\epsilon$ and therefore antiferromagnetic coupling, whereas a

(42) Plass, W.; Pohlmann, A.; Rautengarten, J. *Angew. Chem., Int. Ed.* **2001**, *40*, 4207−4210.
(43) Ginsberg, A. P.; Lines, M. E. *Inorg. Chem.* **1972**, *11*, 2289−2290.
(44) (a) Crawford, V. H.; Richardson, H. W.; Wasson, J. R.; Hodgson, D. J.; Hatfield, W. E. *Inorg. Chem.* **1976**, *15*, 2107−2110. (b) Ruiz, E.; Alemany, P.; Alvarez, S.; Cano, J. *Inorg. Chem.* **1997**, *36*, 3683−3688. (c) Ruiz, E.; Alemany, P.; Alvarez, S.; Cano, J. *J. Am. Chem. Soc.* **1997**, *119*, 1297−1303.
(45) Nishida, Y.; Kida, S. *J. Chem. Soc., Dalton Trans.* **1986**, 2633−2640.
(46) (a) McKee, V.; Zvagulis, M.; Reed, C. A. *Inorg. Chem.* **1985**, *24*, 2914−2919. (b) Thompson, L. K.; Tandon, S. S.; Lloret, F.; Cano, J.; Julve, M. *Inorg. Chem.* **1997**, *36*, 3301−3306.
(47) (a) Kawata, T.; Yamanaka, M.; Ohba, S.; Nishida, Y.; Nagamatsu, M.; Tokii, T.; Kato, M.; Steward, O. W. *Bull. Chem. Soc. Jpn.* **1992**, *65*, 2739−2747. (b) Rodríguez-Fortea, A.; Alemany, P.; Alvarez, S.; Ruiz, E. *Inorg. Chem.* **2002**, *41*, 3769−3778.
(48) Hay, P. J.; Thibeault, J. C.; Hoffmann, R. *J. Am. Chem. Soc.* **1975**, *97*, 4884−4899.
(49) Gehring, S.; Fleischhauer, P.; Paulus, H.; Haase, W. *Inorg. Chem.* **1993**, *32*, 54−60.

folding of the coordination planes reduces $\Delta\epsilon$ and leads to predominant ferromagnetic coupling, which becomes nearly invariant in the region $\tau > 40°$. This behavior was later confirmed by density functional theory (DFT) calculations on dinuclear μ-hydroxo-μ-carboxylato models and explained by the countercomplementarity of the hydroxo and carboxylato bridges.[12] According to the calculations, the antisymmetric combination ϕ'_{AS} is higher in energy in the monohydroxo-bridged model, whereas in the case of the monocarboxylato-bridged model, the symmetric combination ϕ'_{S} is energetically disfavored. In the presence of both bridges, the effects nearly counterbalance each other and the energy gap is reduced to 353 cm^{-1}, resulting in only a weak antiferromagnetic term, which is further reduced upon folding of the coordination planes. As a consequence, the magnetic interactions in μ-hydroxo/alkoxo-μ-carboxylato-bridged copper(II) complexes are usually moderately to weakly antiferromagnetic with small dihedral angles,[45,50] or ferromagnetic in the cases of strongly folded coordination planes.[51]

The observed antiferromagnetic exchange interactions in the present complexes **1** and **2** are relatively weak, which is therefore in accordance with the general behavior of μ-hydroxo/alkoxo-μ-carboxylato-bridged copper(II) complexes and can be explained with the countercomplementary contribution of the different bridging units. However, taking the strong folding of the coordination planes into account, ranging from 62.9 to 69.1°, a ferromagnetic coupling should be expected for both complexes in accordance with the theoretical predictions and experimental results of other studies, as was described above. This prediction is not confirmed by the magnetic data, which reveal an antiferromagnetic interaction. According to the principle of orbital complementarity/countercomplementarity, this indicates that the effects of the two different bridging units are not entirely counterbalanced, resulting in a significant energy gap $\Delta\epsilon$ and a doublet ground state at low temperatures.

A conceivable explanation for the observed antiferromagnetic coupling in **1** and **2** is the Cu−O−Cu angle of the alkoxo bridges. As was mentioned above, it was found in an earlier study that the dihedral angle between the adjacent coordination planes is the decisive structural parameter for the exchange coupling in μ-alkoxo-μ-acetato-bridged copper complexes[49] because the Cu−O−Cu angle and the dihedral angle are correlated. If two adjacent copper centers are placed in a square-planar coordination environment, the Cu−O−Cu angle decreases with an increasing dihedral angle. In the case of our complexes, the coordination geometry of the terminal copper centers is distorted, and therefore the Cu−O−Cu angles are comparatively large, ranging from 111.0 to 113.6°. Taking the well-known correlation between bridging angle and exchange coupling in di-μ-hydroxo- and di-μ-alkoxo-bridged copper complexes into account,[44] this might lead to a larger antiferromagnetic contribution from the alkoxo bridge to the coupling in **1** and **2**, as could be expected solely considering the large dihedral angles between the coordination mean planes.

DFT Calculations. The unusual magnetic properties of **1** and **2** make these complexes good test cases for the ability of DFT to describe the energetics of molecules with a complicated, strongly correlated electronic structure. We carried out DFT calculations on **2**, including all ligands explicitly, employing three density functionals (BP86, B3LYP*, and B3LYP) in combination with Ahlrichs' TZVP basis set (see the Experimental Section for details). The three density functionals differ with respect to a special term in the functional and thus in the resulting potential, which is the so-called exact exchange admixture that has a systematic influence on the energy splittings between different spin states.[34] While BP86 is a pure density functional with no exact exchange, 15 and 20% exact (Hartree−Fock type) exchange are introduced in the B3LYP* and the B3LYP density functionals, respectively. Note that this ingredient of a density functional was identified to be the most crucial term for the calculation of spin-state energy splittings.[34]

As a pure density functional, BP86 can be combined with the computer-time-saving RI density-fitting technique,[31] which was employed for the structure optimization. The structure optimization was carried out in the symmetric $M_S = 0.5$ state (i.e., with a spin sequence of up−down−up on the three copper centers) and for comparison also in the asymmetric $M_S = 0.5$ state using the X-ray crystallographic molecular structure as a starting point in both cases (a geometry gradient norm of 3×10^{-4} hartree/bohr was the convergence criterion). The optimized structure is in reasonable agreement with the X-ray crystallographic structure, in particular with respect to the parameters related to the bridging units (see Table S3 in the Supporting Information for details).

According to the experiments, the electronic ground state of **2** is a doublet. The antiferromagnetic coupling is weak, so the other thermally accessible spin state(s) are only a little higher in energy. Indeed, the DFT total energy calculations with the three different density functionals summarized in Figure 5 confirm these findings qualitatively. The energy differences are too small, however, to allow for an assessment of the contributions from the individual oxygen and acetate bridges onto the spin coupling by an analysis of molecular fragments, as performed in the literature.[12]

The lowest-energy state is always the symmetric doublet with α spin excess on the two terminal copper atoms, Cu1 and Cu2, and β spin excess on the central copper atom, Cu3, with the spin excess corresponding best to one unpaired electron on each copper center. The splittings between the quartet state and the lowest-energy doublet state are small and range from 1.08 (B3LYP) and 1.86 (B3LYP*) to 5.92 kJ mol^{-1} (BP86/RI). The asymmetric doublet state, with β, α, and α spin excess on the copper atoms Cu1, Cu3, and

(50) (a) Bürger, K.-S.; Chaudhuri, P.; Wieghardt, K. *J. Chem. Soc., Dalton Trans.* **1996**, 247−248. (b) Boxwell, C. J.; Bhalla, R.; Cronin, L.; Turner, S. S.; Walton, P. H. *J. Chem. Soc., Dalton Trans.* **1998**, 2449−2450.

(51) (a) McKee, V.; Zvagulis, M.; Dagdigian, J. V.; Patch, M. G.; Reed, C. A. *J. Am. Chem. Soc.* **1984**, *106*, 4165−4712. (b) Tolman, W. B.; Rardin, R. L.; Lippard, S. J. *J. Am. Chem. Soc.* **1989**, *111*, 4532−4533. (c) Nie, H.; Aubin, S. M. J.; Mashuta, M. S.; Porter, R. A.; Richardson, J. F.; Hendrickson, D. N.; Buchanan, R. M. *Inorg. Chem.* **1996**, *35*, 3325−3334. (d) Lee, C.-J.; Cheng, S.-C.; Lin, H.-H.; Wei, H.-H. *Inorg. Chem. Commun.* **2005**, *8*, 235−238.

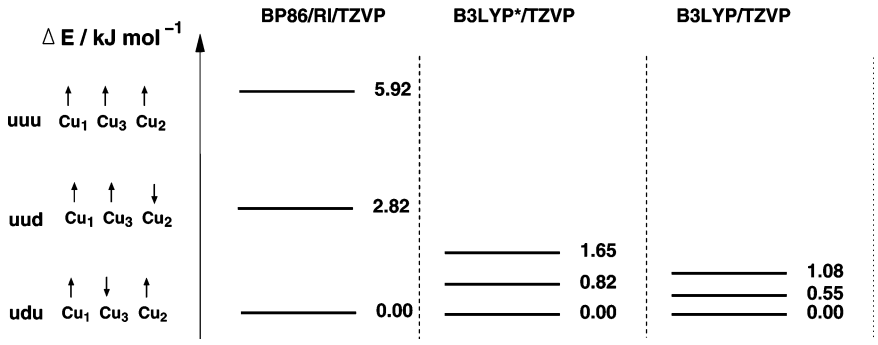

Figure 5. Relative total energies in kilojoules per mole of the three different spin states of **2** as obtained with three different density functionals differing in the admixture of Hartree−Fock-type exact exchange (0% in BP86, 15% in B3LYP*, and 20% in B3LYP). The symmetric doublet state (udu) is taken as a reference (u = up, d = down).

Cu2, respectively, is lying energetically approximately halfway between the symmetric doublet state and the quartet state. These energy splittings are so small that they are below the error margin of contemporary DFT. However, the three density functionals show excellent qualitative agreement and differ only by the well-known dependence of spin-state energy splittings on the exact exchange admixture in the density functional, which usually favors the high-spin state.[34,52] Thus, the qualitative picture appears to be reliable, and the calculations confirm the experimental finding that complex **2** possesses an antiferromagnetically coupled ground state.

An assignment of the calculated DFT energies of the lowest-energy doublet (up−down−up) and quartet (up−up−up) states to the real energies of these states leads to J values of -327 (BP86), -91 (B3LYP*), and -60 cm^{-1} (B3LYP) for **2** by comparison with the energy splitting as derived from eq 1. This is in qualitative agreement with the measured value of -24 cm^{-1}, whereas the quantitative agreement is moderate and depends strongly on the density functional chosen. On the basis of numerous previous studies[34,52] and in view of the very small absolute values of the energy splittings, which are below the general accuracy of contemporary DFT methods, we may recommend the B3LYP* functional as an appropriate reference.

In the Heisenberg model, one assumes to have strictly localized spins on the metal atoms interacting with one another. However, a local spin analysis reveals that the spin excess in the Cu_3 complex **2** is only partially localized on the copper atoms and that a considerable part (about one-third) of it is delocalized over all oxygen and nitrogen atoms directly coordinated to the copper atoms (see Table 4). Therefore, discrepancies between calculations of the Heisenberg coupling constants based on ideal local spin values (which assume no delocalization of the spin excess) and measured coupling constants are not necessarily a sign of a deficiency of the computational method but may as well be due to the possible inappropriateness of a Heisenberg model in this case. For this reason, we do not try to reproduce the experimental coupling constant by adjusting the exact exchange parameter.

Table 4. Local $\langle \hat{S}_{zA} \rangle$ Expectation Values Obtained with Preorthogonalized Löwdin (Löwdin*) Projectors from DFT/B3LYP* Calculations on **2**[a]

	udu	duu	uuu		udu	duu	uuu
Cu1	0.32	−0.32	0.32	O31	0.03	−0.03	0.03
Cu3	−0.34	0.34	0.34	O32	−0.03	0.03	0.03
Cu2	0.32	0.32	0.32	O41	0.03	0.03	0.03
O11	0.05	−0.05	0.05	O42	−0.03	0.04	0.04
O12	0.00	0.00	0.07	N11	0.04	−0.04	0.04
O21	0.05	0.05	0.05	N21	0.04	0.04	0.04
O22	0.00	0.06	0.07				

[a] Note that one unpaired electron on an atom A corresponds to a $\langle \hat{S}_{zA} \rangle$ expectation value of 0.5. That is, the number of excess electrons on atom A is obtained by multiplication of the data in the table with a factor of 2. Note also that a minus sign indicates β excess electrons, while a positive number denotes α excess electrons.

Conclusions

Copper(II) complexes of two new Schiff-base ligands based on the aminosugar 6-amino-6-deoxy-1,2,3-tri-*O*-methyl-α-D-glucopyranoside and two salicylaldehyde derivatives have been synthesized. The resulting complexes reveal a trinuclear structure with two terminal copper−ligand moieties bridged to a central copper atom via two acetate ions and the deprotonated sugar OH groups. Spectroscopic experiments indicate that the trimeric structure of the complexes is maintained in a methanolic solution.

The copper centers show a moderate antiferromagnetic coupling and the temperature dependence of the magnetic susceptibility is in accordance with the assumed model of a symmetric and linear trinuclear spin topology without direct coupling between the terminal copper centers. According to earlier studies, for μ-alkoxo-μ-acetato-bridged copper complexes with rather large dihedral angles between the coordination mean planes, as found in **1** and **2**, the expected magnetic interaction should be ferromagnetic. In this respect, the observed antiferromagnetic exchange coupling is unusual and is possibly caused by the strong distortion of the terminal copper coordination geometries, resulting in relatively large Cu−O−Cu angles for the alkoxo bridges. DFT calculations of complex **2**, applying different density functionals, showed that the electronic ground state is a doublet and therefore confirmed the experimental finding of an antiferromagnetic coupling. Despite the small energy splitting between the

(52) (a) Herrmann, C.; Yu, L.; Reiher, M. *J. Comput. Chem.* **2006**, *27*, 1223−1239. (b) Bruschi, M.; De Gioia, L.; Zampella, G.; Reiher, M.; Fantucci, P.; Stein, M. *J. Biol. Inorg. Chem.* **2004**, *9*, 873−884. (c) Ganzenmueller, G.; Berkaine, N.; Fouqueau, A.; Casida, M. E.; Reiher, M. *J. Chem. Phys.* **2005**, *122*, 234321. (d) Harvey, J. *Struct. Bonding (Berlin)* **2004**, *112*, 151−184.

symmetric doublet, the asymmetric doublet, and the quartet states, all calculations indicate that the symmetric doublet state is the energetically favored one.

Despite the significant differences in the aromatic fragment of the two ligands used in this work, both complexes **1** and **2** show the same structural motif with striking geometric resemblance. This indicates that the formation of such trinuclear complexes might be a general feature of this ligand system in the presence of copper(II) salts and acetate ions, favored by the configuration of the sugar fragment and the resulting alignment of the donor groups. Therefore, this should provide relatively easy access to a variety of new trinuclear complexes, which will be the subject of further studies in our group, especially with respect to their reactivity in catalytic reactions.

Acknowledgment. This work was supported by a grant from the Deutsche Forschungsgemeinschaft [Grants SFB 436 ("Metal-Mediated Reactions Modeled after Nature") and SPP 1137 "Molecular Magnetism")]. The John von Neumann Institut für Computing is acknowledged for its generous support with computing time at the supercomputer center of the Forschungszentrum Jülich (Project "Magnetic Interactions in Transition Metal Complexes"). A.R. gratefully acknowledges the support by a Graduiertenstipendium of the Freistaat Thüringen. M.R. thanks the Fonds der Chemischen Industrie (FCI) for a Dozentenstipendium, and C.H. gratefully acknowledges financial support by the FCI through a Doktorandenstipendium.

Supporting Information Available: Crystallographic details on the modifications of **1**, details on the magnetic analysis of **1**, tables of selected bond angles for **1** and **2** as well as the calculated (DFT) bond distances of **2**, figures of the molecular structure of complex **2** and the V-shaped folded structure of **1**, representation of the vibrational modes of the bridging acetate ligands of **2**, and graphs of the field dependence of the magnetization for **1b** and **2**. This material is available free of charge via the Internet at http://pubs.acs.org.

IC0605064